Article

Gene expression during ER stress–induced apoptosis in neurons: induction of the BH3-only protein Bbc3/PUMA and activation of the mitochondrial apoptosis pathway

Claus Reimertz,[1,2] Donat Kögel,[1,2] Abdelhaq Rami,[3] Thomas Chittenden,[4] and Jochen H.M. Prehn[1,2]

[1]Interdisciplinary Center for Clinical Research, University Münster Clinics, D-48149 Münster, Germany
[2]Experimental Neurosurgery, Center for Neurology and Neurosurgery, and [3]Department of Anatomy III, Johann Wolfgang Goethe University Clinics, D-60590 Frankfurt, Germany
[4]ImmunoGen, Inc., Cambridge, MA 02139

Endoplasmic reticulum (ER) stress has been implicated in the pathogenesis of ischemic and neurodegenerative disorders. Treatment of human SH-SY5Y neuroblastoma cells with tunicamycin, an inhibitor of protein glycosylation, rapidly induced the expression of target genes of the unfolded protein response. However, prolonged treatment also triggered a delayed, caspase-dependent cell death. Microarray analysis of gene expression changes during tunicamycin-induced apoptosis revealed that the Bcl-2 homology domain 3-only family member, Bcl-2 binding component 3/p53 upregulated modulator of apoptosis (*Bbc3/PUMA*), was the most strongly induced pro-apoptotic gene. Expression of Bbc3/PUMA correlated with a Bcl-xL–sensitive release of cytochrome *c* and the activation of caspase-9 and -3. Increased expression of Bbc3/PUMA was also observed in p53-deficient human cells, in response to the ER stressor thapsigargin, and in rat hippocampal neurons after transient forebrain ischemia. Overexpression of Bbc3/PUMA was sufficient to trigger apoptosis in SH-SY5Y neuroblastoma cells, and human cells deficient in *Bbc3/PUMA* showed dramatically reduced apoptosis in response to ER stress. Our data suggest that the transcriptional induction of Bbc3/PUMA may be sufficient and necessary for ER stress–induced apoptosis.

Introduction

An imbalance between the cellular demand for protein synthesis and the capacity of the ER in promoting protein maturation and transport can lead to an accumulation of unfolded or malfolded proteins in the ER lumen. This condition has been designated "ER stress" (Kaufman, 1999). It has been suggested that ER stress contributes to neuronal injury after cerebral ischemia (Paschen and Frandsen, 2001; DeGracia et al., 2002) and may play an important role in the pathogenesis of neurodegenerative disorders such as Parkinson's and Alzheimer's disease (Sherman and Goldberg, 2001).

ER stress provokes a controlled transcriptional response, the unfolded protein response (UPR). Target genes of the UPR include molecular chaperones that help to alleviate ER stress by promoting the correct folding of nascent proteins in the ER and by inhibiting the aggregation of aberrant proteins. However, if ER stress is severe and prolonged, stressed cells will eventually activate an evolutionary conserved, caspase-dependent death program (Perez-Sala and Mollinedo, 1995). In murine cells, ER stress–induced cell death has been shown to involve the activation of ER-resident caspase-12, which subsequently activates executioner caspases such as caspase-3 (Nakagawa and Yuan, 2000; Nakagawa et al., 2000). However, although the role of caspase-12 in ER stress–induced apoptosis of murine cells is well established,

Figure 1. **Tunicamycin induces ER stress and apoptosis in human SH-SY5Y neuroblastoma cells and rat hippocampal neurons.** (A and B) Induction of *BiP* by tunicamycin treatment of SH-SY5Y cells. (A) Kinetics of *BiP* mRNA induction by tunicamycin in SH-SY5Y cells. Cells were treated with 3 μM tunicamycin or vehicle (DMSO) for the indicated times. Total RNA was analyzed by RT-PCR analysis for the expression of BiP and GAPDH. (B) Kinetics of BiP protein expression after tunicamycin treatment of SH-SY5Y cells. Whole-cell extracts were analyzed by Western blot analysis for BiP and α-tubulin protein levels. Similar results were obtained in two independent experiments. (C) Flow cytometric analysis of DNA fragmentation induced by tunicamycin. SH-SY5Y cells were incubated for 24 h with 3 μM tunicamycin or vehicle with or without addition of 200 μM zVAD-fmk. After treatment, cells were harvested, permeabilized, and stained with propidium iodide (FL2-H). Subsequently, cells were analyzed by FACS®. The sub-G1 region is marked with M1. Data from 10,000 cells are shown. (D) Time course of appearance of sub-G1 cells. The percentage of events within the marked region (M1), which represents the apoptotic cell population, was calculated using CellQuest™ software (BD Biosciences). Data are means ± SEM from *n* = 4 separate experiments per time point. Different from control (Con): *, P < 0.05. (E) Time course of tunicamycin-induced caspase-3–like protease activity in SH-SY5Y neuroblastoma cells. Caspase-3–like activity was measured by cleavage of 10 μM fluorogenic substrate Ac-DEVD-AMC. Data are means ± SEM

from *n* = 3 separate experiments. Different from control (Con): *, P < 0.05. (F) Tunicamycin treatment of rat hippocampal neurons leads to the apoptotic phenotype with condensed and fragmented nuclei. Cultures of primary hippocampal neurons were incubated with 3 μM tunicamycin or vehicle for 24 h. Cells were fixed and nuclei were stained with Hoechst 33258. Bar, 25 μm. (G) Quantification of apoptosis in tunicamycin-treated hippocampal neurons. Cultures were incubated with the indicated concentrations of tunicamycin for 24 h. Cells were fixed and stained with Hoechst 33258. Apoptotic nuclei, showing condensed or fragmented chromatin, were counted within three randomly chosen subfields. Data are means ± SEM from *n* = 4–12 cultures in three separate experiments. Different from control (Con): *, P < 0.05.
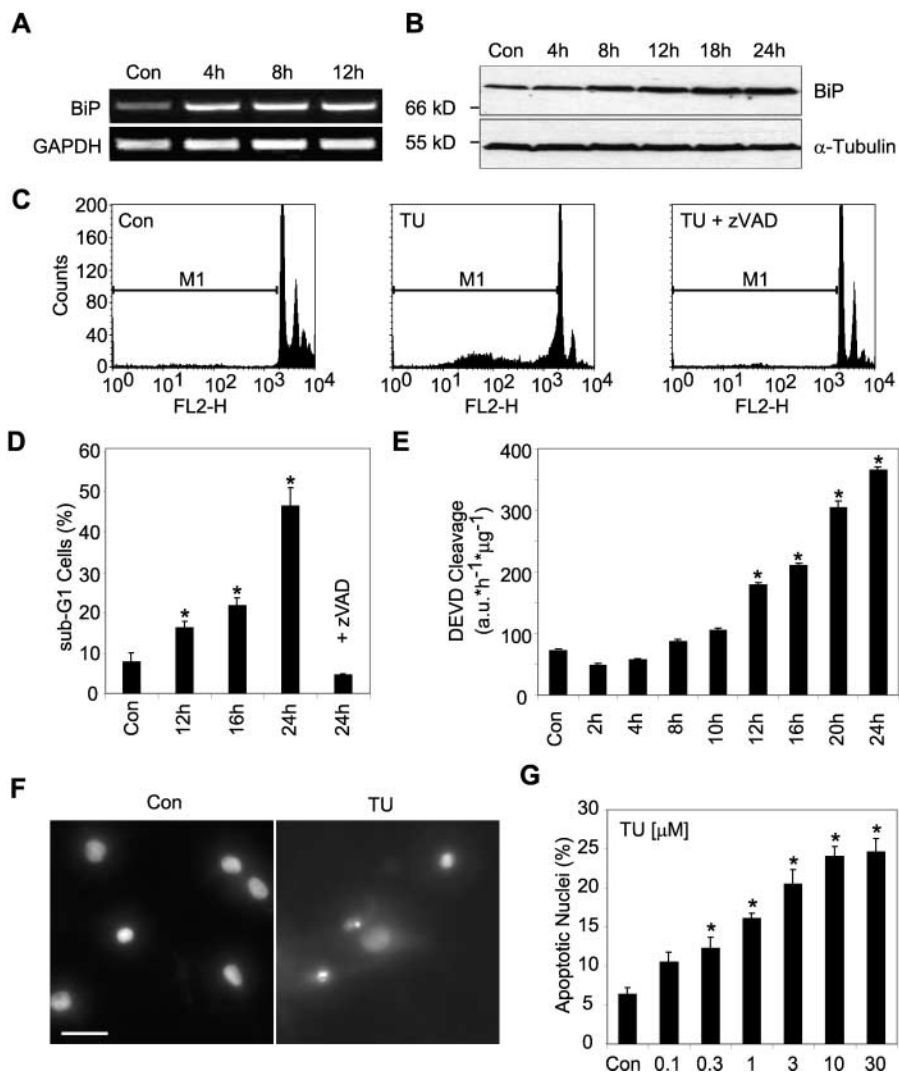
there is also evidence that the human caspase-12 gene is nonfunctional due to the acquisition of inactivating gene mutations (Fischer et al., 2002). This suggests that additional pathways may be important in humans.

Indeed, evidence has been presented that ER stress may activate the mitochondrial apoptosis pathway (Häcki et al., 2000; Annis et al., 2001; Wei et al., 2001). In this pathway, the release of pro-apoptotic factors from mitochondria requires an increase in outer mitochondrial membrane permeability, triggered by the pro-apoptotic Bcl-2 family members Bax and Bak (Desagher and Martinou, 2000; Wei et al., 2001). Both proteins have to undergo a conformational change to trigger this increase. In healthy cells, anti-apoptotic Bcl-2 family members such as Bcl-2 and Bcl-xL inhibit this conformational change. On induction of apoptosis, this inhibition is overcome by the transcriptional induction or posttranslational activation of Bcl-2 ho-

mology domain 3 (BH3)-only proteins (Huang and Strasser, 2000).

In the present work, we used high density oligonucleotide microarrays to analyze gene expression during tunicamycin-induced ER stress in human neural cells, and provide evidence that the transcriptional induction of the BH3-only protein Bcl-2 binding component 3/p53 upregulated modulator of apoptosis (Bbc3/PUMA) activates the mitochondrial apoptosis pathway in response to ER stress.

Results

Tunicamycin induces caspase-dependent apoptosis in neurons

Treatment of human SH-SY5Y neuroblastoma cells with the ER stressor tunicamycin induced mRNA and protein expression of the ER resident molecular chaperone immuno-

globulin heavy chain–binding protein (*BiP*), a known UPR target gene (Fig. 1, A and B). Despite this protective response, prolonged treatment with tunicamycin resulted in apoptotic cell death. FACS® analysis of the DNA content demonstrated that tunicamycin treatment induced a characteristic sub-G1 peak in the human neuroblastoma cells, in-

dicative of DNA fragmentation, a hallmark of apoptosis (Fig. 1 C). After 24 h, ∼50% of cells had a reduced DNA content (Fig. 1 D, sub-G1). Co-incubation with the broad-spectrum caspase inhibitor zVAD-fmk blocked the appearance of sub-G1 cells, indicating that this process was caspase-dependent. Indeed, tunicamycin induced a caspase-

Table I. **Differentially expressed genes after tunicamycin treatment classified into distinct functional subgroups**

Target genes	GenBank/EMBL/DDBJ accession no.	Up-/down-regulated	Course
Protein folding and maturation			
BiP/GRP78	X87949	+	Persistent
Protein disulfide-isomerase–related protein P5	D49489	+	Persistent
Collagen-binding protein 2	D83174	+	Persistent
Fourth mammalian ER DNAJ protein (ERdj4)	AL080081	+	Early
Oxygen-regulated protein 150 kD (ORP150)	U65785	+	Late
FK506-binding protein (FKBP13)	AA158243	+	Late
GRP94	X15187	+	Late
Protein disulfide-isomerase ERp70-like	AI262789	+	Late
Protein disulfide-isomerase ERp60	Z49835	+	Late
Proline 4-hydroxylase, beta subunit (P4HB)	J02783	+	Intermediate
hsc70 (71-kD heat shock cognate protein)	Y00371	−	Intermediate
Protein transport			
Putative mitochondrial inner membrane protein import receptor (hTIM44)	AF026030	+	Persistent
Translocon-associated protein delta subunit (TRAP δ)	Z69043	+	Late
Syntaxin 5	U26648	+	Late
Translocating chain–associating membrane protein (TRAM)	X63679	+	Late
Transmembrane protein rnp24	X92098	+	Late
Protein synthesis and modification			
Glycyl-tRNA synthetase	U09510	+	Persistent
Alanyl-tRNA synthetase	D32050	+	Persistent
Asparagine synthetase	M27396	+	Persistent
Glutamine-fructose-6-phosphate amidotransferase (GFAT)	M90516	+	Intermediate
Integral membrane protein 1 (ITM1)	L38961	+	Late
Ca^{2+} homeostasis			
Calreticulin	AD000092	+	Persistent
Stanniocalcin 2	AF098462	+	Early
Plasma membrane Ca^{2+}-pumping ATPase	J04027	+	Intermediate
Calnexin	L10284	+	Late
Novel DNA-binding/EF-hand/leucine zipper protein (NEFA)	X76732	+	Late
Nucleobindin 1	M96824	+	Late
Transcription factors			
CHOP	S62138	+	Persistent
C/EBP-beta	X52560	+	Persistent
TGF-β–stimulated clone 22 (TSC22)-like	AI635895	+	Persistent
X-box–binding protein 1 (XBP-1)	Z93930	+	Early
Egr-1	X52541	+	Early
UPR target genes of unknown function			
HERP	AF055001	+	Persistent
SERP/RAMP4	AI557272	+	Late
Apoptosis			
Bbc3/PUMA	U82987	+	Intermediate

Expression profiling by microarray analysis after induction of ER stress with tunicamycin. SH-SY5Y neuroblastoma cells were treated with 3 μM tunicamycin for 4, 8, or 12 h. Controls were treated with vehicle (DMSO) for 8 h. cRNA was prepared and hybridized to HG-U95A microarrays, after which relative mRNA levels were quantified with the Affymetrix Microarray Suite 4.1 software (see Materials and methods). GRP78, 78-kD glucose-regulated protein; GRP94, 94-kD glucose-regulated protein; HERP, homocysteine-inducible, ER stress–inducible, ubiquitin-like domain member 1; SERP1/RAMP4, stress-associated ER protein 1/ribosome-associated membrane protein 4; C/EBP-beta, CCAAT/enhancer-binding protein beta. Column 4 (Course) refers to the expression kinetics shown in Fig. 2 A.

3–like protease activity in cytosolic extracts determined by measuring the cleavage of Ac-DEVD-AMC, a fluorogenic substrate preferentially cleaved by caspase-3 and -7 (Fig. 1 E). Treatment with tunicamycin also induced apoptosis in primary cultures of rat hippocampal neurons (Fig. 1 F) reaching a maximum at a concentration of 10–30 μM (Fig. 1 G). Treatment with tunicamycin also led to an early induction of the molecular chaperone BiP in the hippocampal neuron cultures (unpublished data).

Gene expression microarray analysis of tunicamycin-treated SH-SY5Y cells

We used high density oligonucleotide microarrays to analyze gene expression changes during tunicamycin-induced cell death. RNA was isolated from SH-SY5Y neuroblastoma cells treated for 4, 8, or 12 h with 3 μM tunicamycin. A total of 138, 225, and 151 genes were found to be up-regulated after 4, 8, and 12 h of tunicamycin treatment, respectively (see Materials and methods for detailed description of data analysis). The number of down-regulated genes was 100, 69, and 88 after 4, 8, and 12 h, respectively. Table I provides a list of selected, differentially expressed genes after ER stress, sorted into distinct functional subgroups. Column 4 refers to the expression kinetics shown in Fig. 2 A. Expression kinetics were classified into persistent, early, intermediate, or late changes (Fig. 2 A). Increased expression of distinct ER stress–induced genes was confirmed by semiquantitative RT-PCR analysis (Fig. 2 B). A list of all differentially expressed genes is provided in the supplemental material (available at http://www.jcb.org/cgi/content/full/jcb.200305149/DC1).

Genes involved in protein folding

The largest group of up-regulated target genes was represented by ER-resident molecular chaperones and disulfide isomerases. Among the molecular chaperones, we found established UPR target genes such as *BiP*, 94-kD glucose-regulated protein, oxygen-regulated protein 150 (*ORP150*), and the fourth mammalian ER DNAJ protein (*ERdj4*). Other activated genes included disulfide isomerases such as protein disulfide isomerase ER-60 precursor (*ERp60*) and the proline 4-hydroxylase, β subunit (*P4HB*). Protein folding is catalyzed and accelerated by members of the peptidyl prolyl cis/trans isomerase family of which *cyclophilin B* and FK506-binding protein 13 (*FKBP13*) were potently up-regulated by tunicamycin. Interestingly, the expression of the chaperone 71-kD heat shock cognate protein (*hsc70*) was significantly lowered during ER stress. Other chaperones down-regulated on tunicamycin treatment included DNAJ-like 2, the 90-kD heat shock protein, and the 28-kD heat shock protein.

Genes involved in protein transport

The second major group of target genes included genes involved in cotranslational translocation of proteins across the ER membrane and the anterograde/retrograde transport back into the cytosol. This group included the signal recognition particle receptors *SRP54* and *SRP19*, the signal sequence receptors *SSR1* and *4*, members of the SEC61 complex (*SEC61 β* and *γ*, as well as *SEC63*), translocating chain–associating membrane protein (*TRAM*) and translocon-associated protein delta subunit (*TRAP δ*). Up-regulated genes also included genes involved in the anterograde/retrograde transport between ER and Golgi. These were represented by a coated vesicle membrane protein (*rnp24*), a transmembrane trafficking protein (*tmp21*), and *syntaxin 5*. Other up-regulated genes involved in intracellular protein trafficking included the mitochondrial inner membrane translocase *hTIM44*.

Genes involved in protein synthesis

The translational machinery for a new boost of protein synthesis has been suggested to be amplified during UPR-asso-
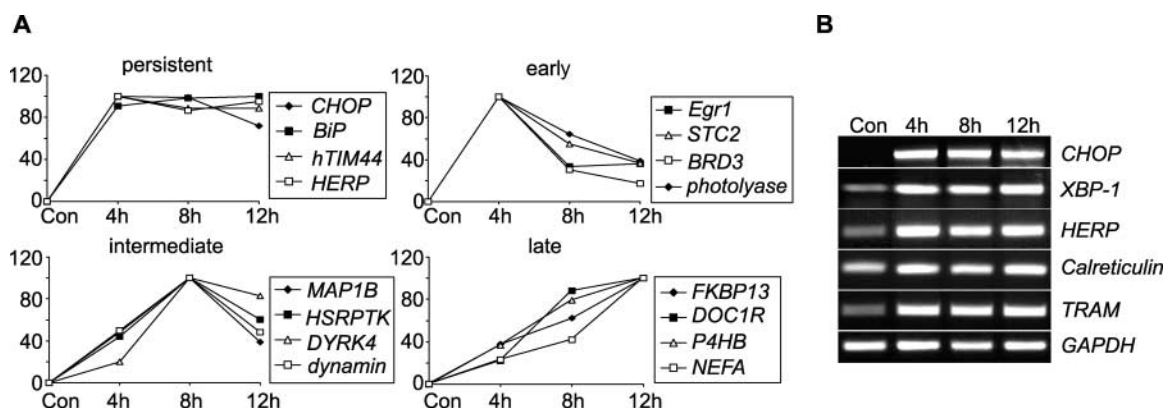
Figure 2.   **Selected tunicamycin-induced genes classified with respect to their expression kinetics.** Expression profiling by microarray analysis after induction of ER stress was performed as described in the legend of Table I. (A) Four representative genes per group were chosen. (B) Confirmation of gene chip data by semiquantitative RT-PCR analysis of five selected genes. *GAPDH* served as control. Similar results were obtained in two separate experiments. *HERP*, homocysteine-inducible, ER stress-inducible, ubiquitin-like domain member 1; STC2, stanniocalcin 2; *BRD3*, bromodomain containing protein 3; *MAP1B*, microtubule-associated protein 1B; HSRPTK, homo sapiens receptor protein tyrosine kinase; *DYRK4*, dual-specificity tyrosine-(Y)-phosphorylation regulated kinase 4; *FKBP13*, 13-kD FK506-binding protein; DOC1R, deleted in oral cancer-related 1; *hTIM44*, putative mitochondrial inner membrane protein import receptor; *P4HB*, proline 4-hydroxylase, beta subunit; *NEFA*, novel DNA-binding/EF-hand/leucine zipper protein; *TRAM*, translocating chain-associating membrane protein; *XBP-1*, X-box–binding protein 1.

ciated translational attenuation (Okada et al., 2002). We observed an up-regulation of eight tRNA synthetase genes after treatment with tunicamycin. Asparagine synthetase, an activating transcription factor 4 (*ATF4*) target gene, was also significantly induced.

Genes regulating Ca²⁺ homeostasis

Members of this group included calreticulin and calnexin. Both proteins regulate ER Ca²⁺ homeostasis, but also function as Ca²⁺-dependent ER chaperones. Genes involved in the regulation of Golgi Ca²⁺ homeostasis included *nucleobindin 1* and novel DNA binding/EF-hand/leucine zipper protein (*NEFA*). Of note, two members of the P-type transport ATPase family, the plasma membrane Ca²⁺ pumping ATPase (*ATP2B1*) and sarcoplasmic reticulum Ca²⁺-ATPase 2 (*ATP2A2*) were also induced.

Transcription factors

Up-regulated transcription factors included two established UPR target genes: C/EBP homologous protein (*CHOP*) and X box–binding protein 1 (*XBP-1*). Both transcription factors were persistently activated with a relatively even expression level at all three time points investigated. *CHOP* showed the largest expression increase of all genes analyzed. Interestingly, expression of the stress-responsive transcriptional regulator early growth response 1 (*Egr-1*) was also significantly enhanced. In addition, the *CHOP* interaction partner CCAAT/enhancer binding protein beta (C/EBP-β) was potently induced.

ER stress induced by tunicamycin activates the BH3-only gene *bbc3/PUMA*

Tunicamycin-induced ER stress also altered the transcription of *bbc3/PUMA*, a member of the BH3-only gene family. Microarray analysis could not detect an altered transcription of other Bcl-2 family members, including the BH-3-only genes *bim*, *bad*, and ATL-derived PMA-responsive peptide (*APR*; human *Noxa*), the pro-apoptotic Bcl-2 family members *bax* and *bak*, and the anti-apoptotic genes *bcl-2* and *bcl-x*. There was a mild induction of *DR5/Trail-R2* (2.1-fold increase after 8 h), but the expression of other genes involved in death receptor–mediated apoptosis including *Fas/CD95/APO-1*, *Fas ligand*, *TRAIL*, and TRAIL-Receptor *DR3*, was not found to be altered.

Northern blot analysis demonstrated that up-regulation of *bbc3/PUMA* expression could be observed 4 h after addition of tunicamycin (Fig. 3 A). Cell lysates of SH-SY5Y cells treated with 3 μM tunicamycin showed elevated Bbc3/PUMA protein levels starting 12 h after onset of treatment (Fig. 3 B, top). Parallel analysis of caspase-3 activation revealed an ensuing appearance of active caspase-3 subunits detected with an antibody predominantly recognizing the p20 subunit (Fig. 3 B, middle). In concordance with the microarray data, we failed to detect significant protein induction of Bim and Bid (Fig. 3 C), two BH3-only proteins previously implicated in stress-induced apoptosis (Bouillet et al., 1999; Plesnila et al., 2001; Putcha et al., 2001; Whitfield et al., 2001).
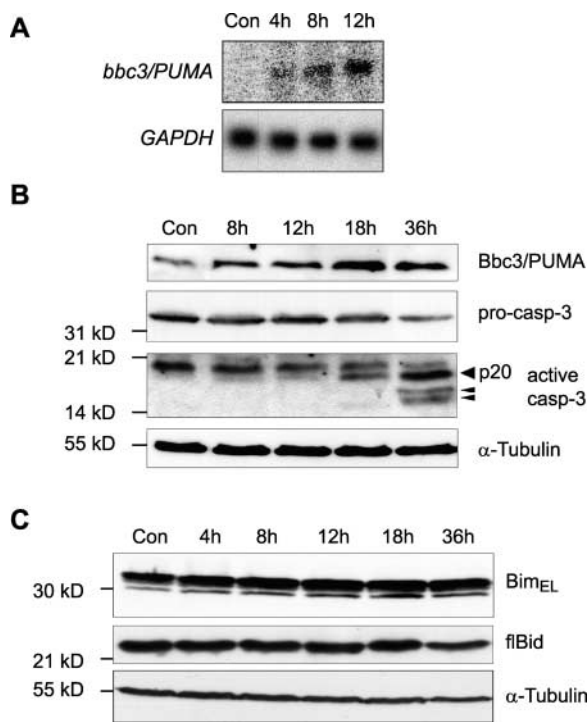
Figure 3. **ER stress induces enhanced Bbc3/PUMA mRNA and protein levels.** (A) Expression of *bbc3/PUMA* mRNA during tunicamycin-induced ER stress in SH-SY5Y neuroblastoma cells determined by Northern blot analysis. (B) Kinetics of Bbc3/PUMA protein expression and caspase-3 activation during tunicamycin-induced cell death in SH-SY5Y neuroblastoma cells. Whole-cell extracts of cells treated for the indicated times with 3 μM tunicamycin or vehicle (DMSO) were analyzed by Western blot analysis. Membranes were probed for either Bbc3/PUMA expression levels or caspase-3 activation. Arrowheads indicate active caspase-3 subunits (p20, p17, and p14). α-Tubulin served as a loading control. Similar results were obtained in two separate experiments. (C) Bim and Bid protein expression during tunicamycin-induced cell death in SH-SY5Y neuroblastoma cells. Cells were treated as described above.
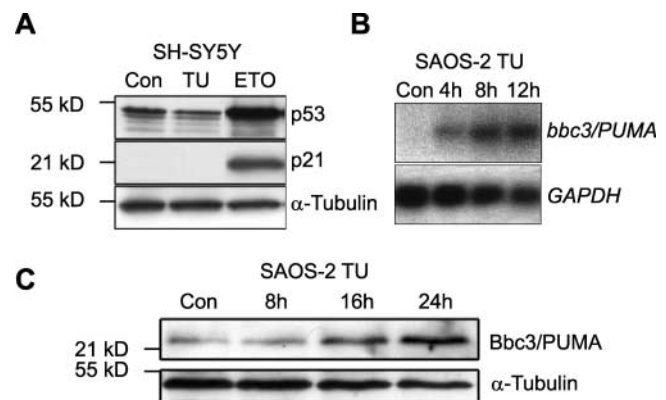
Figure 4. **ER stress is able to induce bbc3/PUMA in a p53-independent manner.** (A) Tunicamycin treatment does not lead to an accumulation of p53 and p21 in SH-SY5Y cells. p53 and p21 protein levels after exposure to tunicamycin (TU; 3 μM, 24 h), etoposide (ETO; 50 μM, 24 h), or vehicle (controls; DMSO, 24 h) were evaluated by Western blotting. (B and C) Kinetics of ER stress–induced *bbc3/PUMA* mRNA and protein levels after 3 μM tunicamycin treatment in p53-deficient human SAOS-2 osteosarcoma cells determined by Northern and Western blot analyses.

Figure 5. **Induction of Bbc3/PUMA is a general cellular response to prolonged ER stress.** (A) Induction of bb33/PUMA mRNA in human SH-SY5Y neuroblastoma cells in response to thapsigargin (TH; 1 μM). Controls (Con) were treated with vehicle (DMSO, 24 h). (B) Bbc3/PUMA protein is expressed in primary hippocampal neurons after tunicamycin treatment. Cultures were treated for 24 h with 3 μM tunicamycin or vehicle. An unspecific band of ∼24 kD served as loading control. (C) Top, increased expression of the ER stress–specific transcription factor CHOP detected by immunohistochemistry in the selective vulnerable CA1 hippocampal subfield of rats subjected to transient forebrain ischemia (Isch). Increased expression of CHOP was detectable as early as 1 h postischemia. Bottom, expression of Bbc3/PUMA is increased in dying CA1 hippocampal pyramidal neurons 5 d after transient forebrain ischemia. Sham-operated animals served as respective controls. Bar, 25 μm. (D) Western blot analysis of Bbc3/PUMA expression in hippocampus and neocortex tissue homogenates 72 h after transient forebrain ischemia (Isch) or sham surgery (Con). Similar results were obtained in a second experiment.
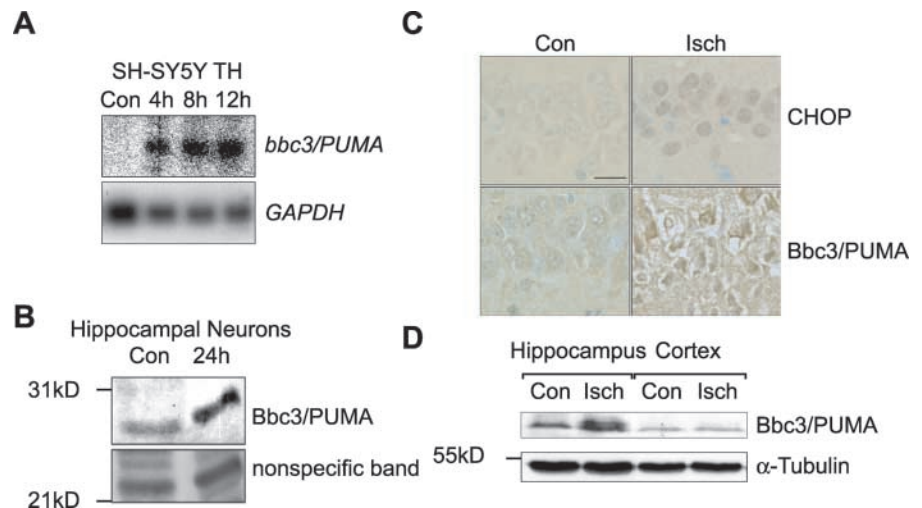
Induction of Bbc3/PUMA is a general, p53-independent cellular response to prolonged ER stress

bbc3/PUMA has been described as a *p53* target gene (Han et al., 2001; Nakano and Vousden, 2001; Yu et al., 2001). However, the microarray data did not reveal significant induction of classical p53 target genes such as *p21* and human *mdm2*. Although Western blot analysis demonstrated significant p53 accumulation and p21 protein induction in SH-SY5Y cells treated with the topoisomerase II inhibitor etoposide, tunicamycin treatment had no effect on p53 and p21 protein levels (Fig. 4 A). Moreover, tunicamycin increased *bbc3/PUMA* mRNA and protein levels in p53-deficient human SAOS-2 osteosarcoma cells (Fig. 4, B and C).

bbc3/PUMA mRNA (Fig. 5 A) and protein (unpublished data) levels also increased in SH-SY5Y neuroblastoma cells exposed to the ER Ca^{2+} ATPase inhibitor thapsigargin, demonstrating that the activation of *bbc3/PUMA* was observed after treatment with a second, pharmacologically distinct ER stressor. Tunicamycin also increased the expression of Bbc3/PUMA in cultured rat hippocampal neurons (Fig. 5 B), demonstrating that the activation of *bbc3/PUMA* was not restricted to transformed human cells.

Cerebral ischemia is a pathophysiological ER stressor (Paschen and Frandsen, 2001; DeGracia et al., 2002). In male Wistar rats subjected to 10 min of forebrain ischemia, increased nuclear accumulation of the transcription factor *CHOP* could be detected in hippocampal pyramidal neurons of the CA1 subfield as early as 1 h after ischemia (Fig. 5 C, top), indicating that ischemia/reperfusion injury induced a rapid ER stress response in selectively vulnerable brain regions. Expression of Bbc3/PUMA was not detectable during the first 24 h after transient forebrain ischemia, but increased expression of CHOP could still be observed (unpublished data). However, expression of Bbc3/PUMA increased significantly in CA1 neurons 48–120 h after ischemia (Fig. 5 C, bottom). This correlated with the onset of neuronal degeneration (Fig. 5 C) and the occurrence of

TUNEL-positive nuclei in the CA1 hippocampal pyramidal cells (Rami et al., 2000). Western blot analysis of the hippocampus and neocortex tissue of ischemic and sham-operated animals 72 h after surgery also provided evidence for a significant induction of Bbc3/PUMA expression in the selectively vulnerable hippocampus (Fig. 5 D).

Activation of the mitochondrial apoptotic pathway during tunicamycin-induced apoptosis

Activation of *bbc3/PUMA* suggested that the mitochondrial apoptosis pathway was activated during ER stress–induced apoptosis. Indeed, treatment with tunicamycin led to Bax activation and clustering in SH-SY5Y neuroblastoma cells, as demonstrated by immunofluorescence analysis using an antibody that specifically detects a conformational change in the Bax protein required for its pro-apoptotic activity (Fig. 6 A). Cells exhibiting Bax clustering showed apoptotic morphology and increased chromatin condensation. Cells with increased chromatin condensation also lost their typical filamentous cytochrome *c* staining (Fig. 6 B), indicating that cytochrome *c* was released from mitochondria. Of note, the apoptotic phenotype of SH-SY5Y cells was always associated with markedly enhanced Bbc3/PUMA immunostaining. Tunicamycin treatment also led to activation of caspase-9, the apical caspase in the mitochondrial apoptosis pathway (Fig. 6 C).

Subsequently, we investigated the effect of Bcl-xL overexpression on tunicamycin-induced apoptosis using SH-Neo and SH-Bcl-xL cells (Luetjens et al., 2001). SH-Neo and SH-Bcl-xL cells responded with increased expression of Bbc3/PUMA and BiP to an exposure to 3 μM tunicamycin (Fig. 6 D; unpublished data). Selective digitonization of the plasma membrane and subsequent immunoblotting experiments revealed that tunicamycin induced a significant accumulation of cytochrome *c* in the cytosol in SH-Neo cells (Fig. 6 E). 3 μM staurosporine (STS) also induced a promi-
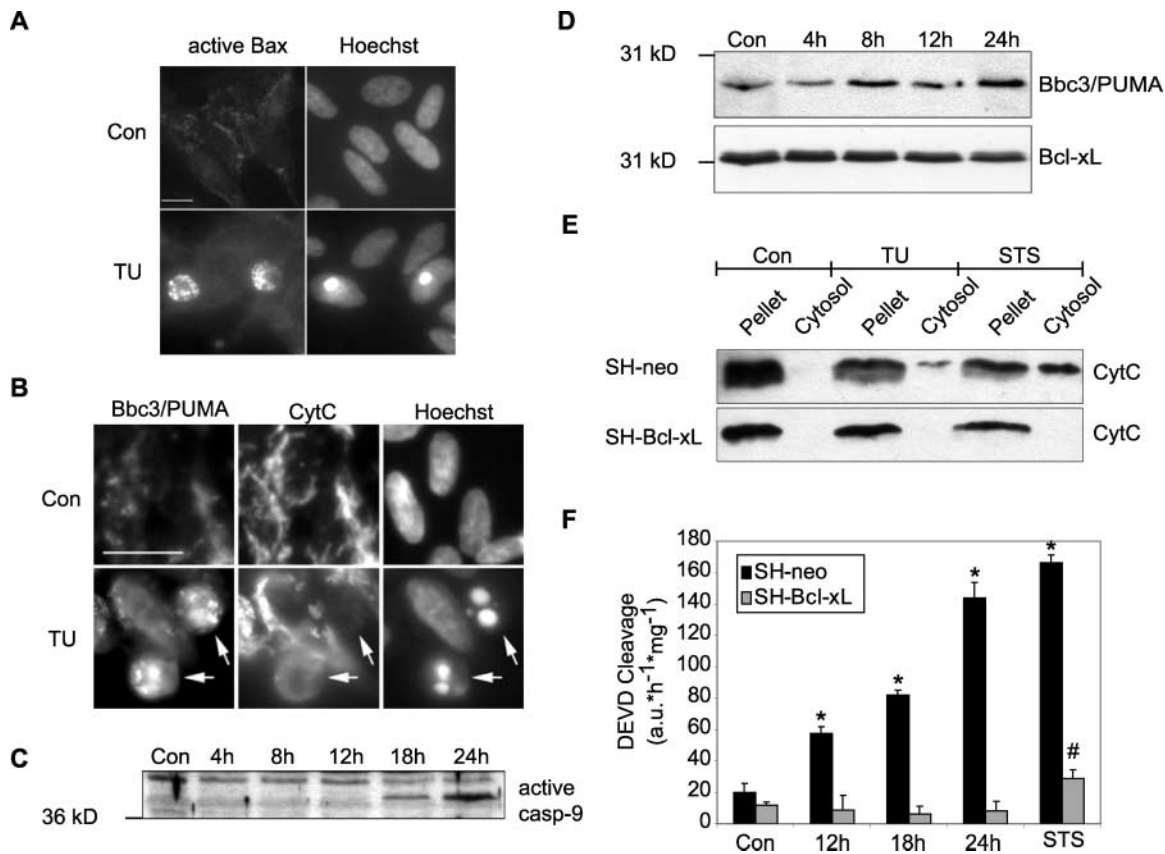
Figure 6. **Tunicamycin activates the mitochondrial apoptosis pathway.** (A) Tunicamycin (TU) treatment activates Bax and induces chromatin condensation. Human SH-SY5Y neuroblastoma cells were exposed to 3 μM tunicamycin or vehicle (Con) for 24 h. Distribution of active Bax and nuclear staining with Hoechst 33258 was analyzed by immunofluorescence microscopy. Bar, 25 μm. (B) High level Bbc3/PUMA expression correlated with cytochrome c release in tunicamycin-treated SH-SY5Y cells. Cells were exposed to DMSO (Con) or 3 μM tunicamycin (TU) for 24 h. Immunofluorescence analysis of Bbc3/PUMA expression and cytochrome c (CytC) redistribution, as well as nuclear staining with Hoechst 33258 was analyzed by epifluorescence microscopy. Arrows indicate cells that have a high expression level of Bbc3/PUMA, a diffuse cytochrome c fluorescence signal indicative of mitochondrial cytochrome c release, and condensed and fragmented chromatin. Bar, 50 μm. (C) Kinetics of caspase-9 activation after tunicamycin-induced apoptosis in SH-SY5Y cells. Whole-cell extracts of cells treated for the indicated times with 3 μM tunicamycin or 24 h with DMSO (Con), were analyzed by Western blotting. Activation of caspase-9 was performed with a rabbit pAb recognizing the 37-kD active subunit. An unspecific band of ∼40 kD serves as a loading control. (D) Induction of Bbc3/PUMA protein expression after tunicamycin treatment is not inhibited in cells overexpressing Bcl-xL. Cell lysates of SH-Bcl-xL cells, incubated with 3 μM tunicamycin for the indicated times or for 24 h with the vehicle (Con) were subjected to Western blot analysis. Bcl-xL expression level served as loading control (bottom). Similar results were obtained in a separate experiment. (E) Tunicamycin induces cytochrome c release in SH-SY5Y cells, which is inhibitable by overexpression of *Bcl-xL*. SH-SY5Y cells stably transfected with an empty vector (SH-neo) or Bcl-xL (SH-Bcl-xL) were incubated for 24 h with vehicle (Con), 3 μM tunicamycin (TU), or for 6 h with 3 μM of the kinase inhibitor staurosporine (STS). Subsequently cells were subjected to controlled digitonin permeabilization of the plasma membrane. Pellets and cytosolic fractions were analyzed by Western blot analysis for cytochrome c levels. (F) Time course of caspase-3–like protease activity in SH-neo and SH-Bcl-xL cells after tunicamycin treatment. Cells were treated for the indicated times with 3 μM tunicamycin, for 24 h with the vehicle DMSO (Con), or for 12 h with 0.1 μM staurosporine (STS). Cytosolic protein extracts were prepared and their caspase-3–like protease activity was determined by measuring the cleavage of the fluorogenic substrate Ac-DEVD-AMC (10 μM). Data are means ± SEM from $n = 4$ separate experiments per time point. *, $P < 0.05$, difference from vehicle-treated control (Con); #, $P < 0.05$, difference from control cell line SH-neo.

nent release of cytochrome c into the cytosol of SH-Neo cells. This release was more pronounced than the release triggered by tunicamycin. However, in direct comparison with tunicamycin, exposure to STS also led to a more rapid and extensive cell death (>80% cell death after 18 h; Luetjens et al., 2001). Interestingly, both tunicamycin- and STS-induced release of cytochrome c release could not be observed in cells overexpressing Bcl-xL. Overexpression of Bcl-xL also potently inhibited the activation of caspase-3–like proteases (DEVDases) in response to tunicamycin and STS (Fig. 6 F).

Expression of *bbc3/PUMA* may be sufficient and required for ER stress–induced apoptosis in human cells

To test whether expression of *bbc3/PUMA* was sufficient to kill human SH-SY5Y neuroblastoma cells, cells were co-transfected with a plasmid encoding EGFP (pEGFP) and either hemagglutinin (HA)-tagged Bbc3/PUMA (pHA-Bbc3/PUMA) or empty vector (pcDNA3.1). Hoechst 33258 staining and morphological analysis of GFP-positive cells demonstrated that bbc3/PUMA-transfected cells revealed morphological characteristics of apoptosis, including cell

Figure 7. **Expression of bbc3/PUMA may be sufficient and required for ER stress–induced apoptosis in human cells.** (A) Transient transfection of SH-SY5Y neuroblastoma cells with bbc3/PUMA leads to induction of apoptosis. Cells were cotransfected with expression plasmids encoding enhanced GFP (pEGFP) and either a hemagglutinin-tagged (HA) version of bbc3/PUMA (pHA-PUMA) or empty vector (pcDNA3.1). 12 h after transfection, cells were fixed and stained with Hoechst 33258. Arrowheads point to transfected cells with the apoptotic phenotype. Similar results were obtained in a separate experiment. (B) Quantitative FACS® analysis of PI uptake of EGFP-positive SH-SY5Y cells transiently cotransfected with expression vectors encoding hemagglutinin-tagged (HA) versions of Bbc3/PUMA, Bbc3/PUMA-ΔBH3, or empty vector (pcDNA3.1). Data were normalized to EGFP-only transfected controls and represent 10,000 events each. For evaluation of comparable transfection rates, whole-cell extracts of cells harvested 16 h after transfection were analyzed by Western blotting. Blots were probed with an anti-hemagglutinin or anti-α-tubulin antibody as loading control. (C) Protein levels of BiP, Bbc3/PUMA, and α-tubulin in human HCT116 control and Bbc3/PUMA-deficient cells treated with 1 μM thapsigargin or vehicle for the indicated time points. (D) FACS® analysis of sub-G1 cells of human HCT116 control and Bbc3/PUMA-deficient cells exposed to 1 μM thapsigargin (TH) or vehicle for 36 h. (E) Quantitative FACS® analysis of thapsigargin- and STS (3 μM)-induced apoptosis. Data from 10,000 events each are means $\pm$ SEM from $n = 3$ separate experiments per time point.
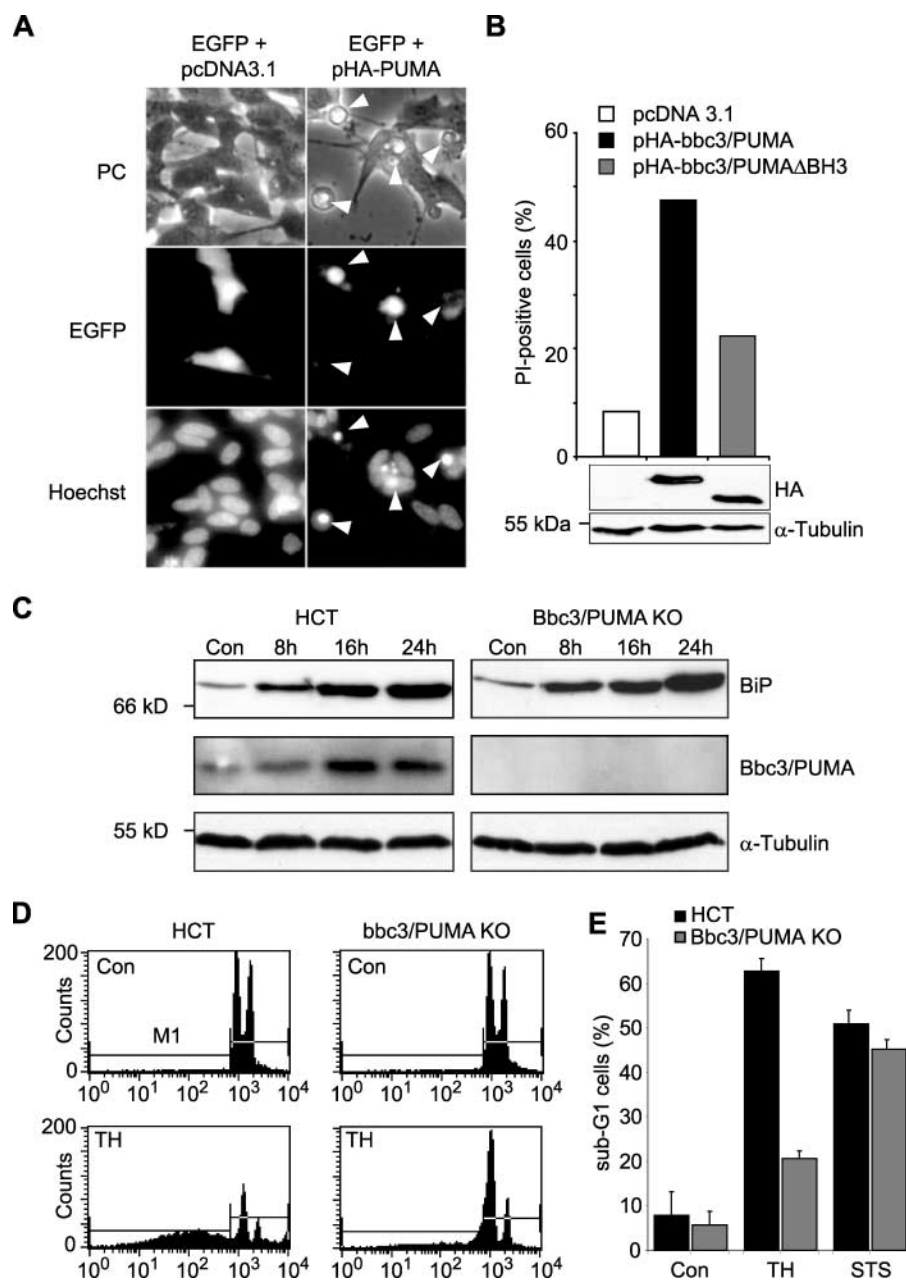
shrinkage and chromatin condensation/fragmentation 16 h after transfection (Fig. 7 A). In contrast, empty vector-transfected controls remained morphologically largely intact. Quantitative FACS® analysis of propidium iodide of EGFP-positive SH-SY5Y neuroblastoma cells transiently cotransfected with expression plasmids encoding either HA-tagged bbc3/PUMA (pHA-bbc3/PUMA), HA-tagged bbc3/PUMA with a deletion in the BH3-domain (pHA-bbc3/PUMA-ΔBH3), or empty vector (pcDNA3.1) demonstrated prominent cell death in bbc3/PUMA-transfected cells, reduced cell death in bbc3/PUMA-ΔBH3–transfected cells (Han et al., 2001), and little cell death in empty vector-transfected cells (Fig. 7 B). Parallel Western blot analysis using an anti-HA antibody showed comparable transfection rates in the pHA-bbc3/PUMA– and pHA-bbc3/PUMA-ΔBH3–transfected cells (Fig. 7 B).

To investigate whether Bbc3/PUMA induction was required for ER stress–induced apoptosis in human cells, we exposed HCT116 control cells and HCT116 cells with targeted disruptions of both alleles of the *bbc3/PUMA* gene (Yu et al., 2003) to the ER stressor thapsigargin (1 μM). Western blot analysis demonstrated a comparable induction of the UPR target gene product BiP in response to thapsigargin in control and Bbc3/PUMA-deficient cells (Fig. 7 C). HCT116 control cells also showed significant induction of Bbc3/PUMA protein in response to thapsigargin. Interestingly, FACS® analysis of DNA content in HCT116 control and Bbc3/PUMA-deficient cells exposed to thapsigargin demonstrated significantly reduced apoptosis in the Bbc3/PUMA-deficient cells (Fig. 7, D and E), whereas the response to STS was not altered (Fig. 7 E).

Discussion

ER stress response and protein quality control

In this analysis, we have used high density oligonucleotide microarrays to analyze transcriptional changes during ER stress–induced apoptosis in human SH-SY5Y neuroblastoma cells. Among the early and persistently induced genes, we found genes that relieve ER stress by promoting protein folding and by keeping proteins in a folding-competent state. This group was represented by molecular chaperones of the classical (*BiP, GRP94*) and nonclassical (lectin-like molecular chaperones like *calnexin* and *calreticulin*) type, along with protein disulfide isomerases. Also, we observed the induction of the sarcoplasmic reticulum Ca^{2+}-ATPase 2 *ATP2A2* (SERCA2) and the plasma membrane Ca^{2+} pumping ATPase (*ATP2B1*). Up-regulation of SERCA2 has previously been observed in response to different ER stressors (Hojmann Larsen et al., 2001). Up-regulation of both plasma membrane- and ER-localized Ca^{2+}-ATPases may help to relieve ER stress by refilling of ER Ca^{2+} stores.

A distinct group of genes differentially regulated by tunicamycin is involved in cotranslational translocation of proteins across the ER membrane, protein trafficking to other organelles such as mitochondria, and proteins involved in retrograde transport back into the cytosol. With the exception of translocating chain–associating membrane protein, this group of genes was induced late during ER stress. Induction of members of the SEC61 complex may link the UPR with ER-associated degradation (ERAD; Wiertz et al., 1996; Plemper et al., 1997). Hence, ER stress may result in a highly ordered gene regulation process comprised of different sequential steps: an early up-regulation of molecular chaperones in order to keep nonglycosylated proteins in a folding-competent state, followed by an improvement of the capacity of the secretory pathway. If ER stress persists, the ERAD pathway may be switched on to target unfolded proteins to degradation via the proteasome.

Transcriptional regulation of ER stress

The transcription factor *CHOP* was the gene most strongly induced by tunicamycin. In overexpression studies, *CHOP* has been shown to negatively regulate cell cycle and induce apoptosis (Barone et al., 1994; Zinszner et al., 1998). The transcription factor *C/EBP-β*, an interaction partner of *CHOP*, was also strongly up-regulated during ER stress. *CHOP* acts as a dominant-negative regulator of C/EBPs and inhibits the DNA-binding activity of C/EBP-β by forming heterodimers that cannot bind DNA (Ron and Habener, 1992). Therefore, CHOP may have a dual function; first acting as an inhibitor of C/EBP proteins to activate distinct target genes, and second, as a direct activator of CHOP target genes (Ubeda et al., 1996). Notably, we could not detect increased expression of known "downstream of CHOP" (doc) genes (Wang et al., 1998) such as homologues of the actin-binding proteins villin and gelsolin and carbonic anhydrase VI (*CA-VI*). This suggests that *CHOP* does not function independently of other transcription factors (like C/EBP-β) during ER stress, and favors the idea that transcription is limited to genes activated by heterodimers of CHOP-C/EBP-β. We also observed the potent induction of the transcription factor *Egr-1*, which was activated early and transiently after ER stress. *Egr-1* has been shown to be induced as an "immediate-early gene" during several physiological and pathophysiological stress conditions, including ischemia (Yan et al., 2000). *Egr-1* has previously been linked to cell death induced by the ER Ca^{2+} ATPase inhibitor thapsigargin, and has been shown to induce apoptosis in human melanoma cells (Muthukkumar et al., 1995).

ER stress and apoptosis

There are two possible outcomes of prolonged ER stress: (1) an adaptive response promoting cell survival; or (2) the induction of apoptotic cell death. Among the pro-apoptotic genes, the BH3-only gene *bbc3/PUMA* was significantly up-regulated after prolonged tunicamycin treatment. *Bbc3/PUMA* was likewise up-regulated after an exposure to thapsigargin, which induces ER stress by depleting ER Ca^{2+} stores. *bbc3/PUMA* has previously been identified as a p53 target gene (Nakano and Vousden, 2001; Yu et al., 2001). However, induction of bbc3/PUMA has also been shown to involve p53-independent regulation (Han et al., 2001). Our results demonstrate that the induction of *bbc3/PUMA* links the cellular ER stress response to the mitochondrial apoptosis pathway, and that this may occur independently of p53. Of note, human cells deficient in Bbc3/PUMA showed dramatically reduced apoptosis in response to ER stress. Interestingly, they still maintained a very low level of apoptosis (Fig. 7 E), suggesting that the (posttranslational) activation of alternative BH3-only proteins or mitochondria-independent apoptosis pathways may only partially compensate for a Bbc3/PUMA deficiency. Induction of Bbc3/PUMA was also observed in primary neuron cultures and in response to cerebral ischemia in vivo, suggesting that regulation of *bbc3/PUMA* expression is a common pathway during ER stress–induced cell death in mammals. Our finding that BH3-only family members are also involved in apoptotic signaling originating from the ER emphasizes the importance and diversity of this gene family in cellular life and death decisions.

Materials and methods

Materials

Tunicamycin, thapsigargin, etoposide, and STS were purchased from Qbiogene. Caspase substrate acetyl-DEVD-7-amido-4-methylcoumarin (Ac-DEVD-AMC) and the broad-spectrum caspase inhibitor Z-Val-Ala-Asp(O-methyl)-fluoromethylketone (zVAD-fmk) were obtained from Bachem. Hoechst 33258 was purchased from Sigma-Aldrich.

Cell lines, cell culture, and transfections

Human SH-SY5Y neuroblastoma cell lines were grown in RPMI 1640. The generation of SH-SY5Y neuroblastoma cells stably overexpressing Bcl-xL (SH-Bcl-xL) or stably transfected with the empty vector (SH-neo) has been described previously (Luetjens et al., 2001). Human SAOS-2 osteosarcoma cells completely lacking expression of endogenous p53 were grown in DMEM culture medium. HCT116 control and Bbc3/PUMA knock-out cells (provided by Drs. B. Vogelstein, L. Zhang, and J. Yu, Johns Hopkins Oncology Center, Baltimore, MD) were maintained in McCoy's 5A medium. All media were supplemented with 10% (vol/vol) FCS, 100 U/ml penicillin, and 100 μg/ml streptomycin (Invitrogen). Primary cultures of hippocampal neurons were prepared from neonatal postnatal day 1 (P1) Fischer 344 rats as described previously (Luetjens et al., 2001). Experiments were performed on 10- to 14-d-old cultures. Animal care followed official governmental guidelines.

For transient transfections, SH-SY5Y cells were plated onto 6-well plates (Nunc). 1 d later, cells were transfected with plasmids encoding HA-

tagged, full-length bbc3/PUMA expression vector (pHA-bbc3/PUMA), HA-tagged, bbc3/PUMA expression vector with a deletion of the BH3 domain (pHA-bbc3/PUMA-ΔBH3; provided by Dr. B. Vogelstein), an expression vector for eGFP (pEGFP-C1; CLONTECH Laboratories, Inc.), or empty vector (pcDNA3.1; Invitrogen) using LipofectAMINE™ transfection reagent (Invitrogen). Transfection procedure was followed as described before (Poppe et al., 2002).

Microarray analysis
SH-SY5Y neuroblastoma cells were treated with tunicamycin or vehicle (0.1% DMSO), harvested, and total RNA was extracted using the RNeasy Midi Kit (QIAGEN). cDNA was synthesized from 40 μg of the total RNA by using the SuperScript™ Choice Kit (Invitrogen). The cRNA was prepared and biotin labeled by in vitro transcription (Enzo Biochemical). Labeled cRNA was fragmented and hybridized for 16 h at 45°C to an HG-U95A array (Affymetrix, Inc.). After hybridization, the gene chips were automatically washed and stained with streptavidin-phycoerythrin by using a fluidics station (GeneChip Fluidics Station 400; Affymetrix, Inc.). Finally, probe arrays were scanned at a 3-μm resolution using the Genechip System confocal scanner (Aligent Technologies). Microarray Suite 4.1 (Affymetrix, Inc.) was used to scan and analyze the relative abundance of each gene from the average difference of intensities. Analysis parameters used by the software were set to values recommended by Affymetrix, Inc (SDT = 4.0, SRT = 1.5). All chip data were normalized to a target intensity of 1000. For each individual gene, the signal ratio between perfect match and mismatch probe cells was used to determine its "Absolute Call," indicating whether the corresponding transcript was present (P), absent (A), or marginal (M). For analysis of differential target gene expression, the "Difference Call Decision Matrix" was used. Individual transcript levels were ranked as either increased (I), marginally increased (MI), decreased (D), marginally decreased (MD), or not changed (NC). To be considered as differentially regulated, the Difference Call of individual transcripts had to be increased/decreased or marginally increased/marginally decreased at the respective time point after treatment with tunicamycin, whereas the Absolute Call had to be present or marginal at the respective time point (up-regulated genes) or in the control (down-regulated genes). A list of all differentially regulated genes meeting this criteria is provided in the online supplemental materials (available at http://www.jcb.org/cgi/content/full/jcb.200305149/DC1). Genes were also classified according to their expression kinetics. The highest fold-induction in comparison to control was set to 100%. Genes up- and down-regulated to at least 50% for all three time points were considered to be persistently regulated. In all other cases, genes were ranked as early (4 h), intermediate (8 h), or late (12 h), depending on the time point when the maximal change of the corresponding transcript was reached. The output from the microarray analysis was merged with the Unigene or GenBank descriptor and stored as an Excel (Microsoft) data spreadsheet. For confirmation of gene chip data, a replication experiment with a second set of independent samples was performed, revealing similar results.

Digitonization
The release of cytochrome *c* from mitochondria was analyzed by a modified selective digitonin permeabilization method that was described previously (Wobser et al., 2002).

SDS-PAGE and Western blotting
Preparation of cell lysates, Western blotting, and immunodetection was performed as described previously (Poppe et al., 2002). The blots were incubated with a mouse monoclonal anti-BiP antibody (SPA 827; StressGen Biotechnologies) diluted 1:1,000, a mouse monoclonal anti-Bbc3 antibody (KM140; Han et al., 2001) diluted 1:1,000, a rat monoclonal Bim antibody (clone 14A8; Qbiogene) diluted 1:1,000, a rabbit polyclonal Bid antibody (#2315-PC; Trevigen) diluted 1:1,000, a rabbit polyclonal p53 antibody (NCL-p53-CM1; Loxo) diluted 1:1,000, a mouse monoclonal p21/WAF antibody (Ab-4, #OP 76; Oncogene Research Products) diluted 1:500, a mouse monoclonal cytochrome *c* antibody (clone 7H8.2C12; BD Biosciences) diluted 1:1,000, a rabbit polyclonal anti-caspase-3 antibody (H-277; Santa Cruz Biotechnology, Inc.) diluted 1:1,000, a rabbit polyclonal anti-caspase-9 antibody (#556585; BD Biosciences) diluted 1:1,000, a mouse monoclonal anti-hemagglutinin (HA) antibody (12CA5; Roche) diluted 1:1,000, or a mouse monoclonal anti-α-tubulin antibody (DM 1A; Sigma-Aldrich), diluted 1:20,000.

RT-PCR
Validation of up-regulated target gene expression was performed by RT-PCR analysis for selected genes. We designed unique oligonucleotide primer pairs by using PRIMER3 software (www.genome.wi.mit.edu/cgi-bin/primer/primer3_www.cgi). Primer sequences are available on request from the authors. Total RNA, purified from tunicamycin-treated cells using the RNeasy Mini kit (QIAGEN), was subjected to RT-PCR in a two-step protocol using M-MLV reverse transcriptase (Invitrogen) and Taq polymerase (Eppendorf; Kögel et al., 2003). The number of cycles and annealing temperature was adjusted depending on the genes amplified.

Northern blot analysis
Total RNA was isolated using the RNeasy Mini or Midi Kit (QIAGEN). 10 μg RNA was subjected to gel electrophoresis on 1.1% formaldehyde/1.2% agarose gels and transferred to nylon membranes (Amersham Biosciences). After UV cross-linking and prehybridization in 50% formamide, 5× SSC, 5× Denhardt's solution, and 1% SDS, pH 7.4, at 65°C for 30 min, the blots were hybridized with an $\alpha[^{32}P]$dCTP-labeled full-length human bbc3/PUMA cDNA probe (Han et al., 2001) and a 700-bp fragment of human glyceraldehyde-3-phosphate dehydrogenase (GAPDH) in 50% formamide, 5× SSC, 5× Denhardt's solution, and 1% SDS, pH 7.4, at 47°C, and were washed according to standard procedures. Membranes were exposed to X-ray film for 24 to 72 h.

Flow cytometry analysis
The measurement of propidium iodide uptake and DNA leakage from apoptotic nuclei and was performed as described previously (Poppe et al., 2002).

Determination of caspase-3–like protease activity
Caspase-3–like protease activity of cells exposed to tunicamycin or vehicle was determined as described before (Poppe et al., 2002).

Transient forebrain ischemia
Transient forebrain ischemia was performed in male Wistar rats (250–300 g; Smith et al., 1984). Cerebral ischemia was induced by clamping both common carotid arteries and lowering the mean arterial blood pressure to 40 mm Hg. After 10 min ischemia, the blood pressure was restored by re-infusion of blood and removal of the clamps. Arterial pH, pCO_2, pO_2, arterial blood pressure, and plasma glucose concentration were determined 15 min before and 15 min after the induction of ischemia. Sham-operated rats served as controls. Animal care followed official governmental guidelines.

Immunohistochemistry
At different time points after cerebral ischemia, rats were anaesthetized with 3.5% halothane and perfused transcardially with phosphate buffer (pH 7.4) containing 4% formaldehyde. The sections were deparaffinized, washed, and subjected to histochemical analysis as described previously (Rami et al., 2000). Sections were incubated with an mAb against CHOP (sc-7351, Santa Cruz Biotechnology, Inc.) diluted 1:10, or a pAb against Bbc3/PUMA (provided by Dr. Karen Vousden (Beatson Institute for Cancer Research, Glasgow, UK; Nakano and Vousden, 2001) diluted 1:50 overnight at 4°C. The immunoreaction was developed with 3,3'-DAB tetrahydrochloride and hydrogen peroxide. Sections were counterstained with cresyl violet.

Immunofluorescence analysis and Hoechst staining
Tunicamycin-treated cells were washed, fixed with 4% PFA, and permeabilized. A rabbit polyclonal anti-Bax antibody specifically recognizing active Bax (Desagher et al., 1999; #06–499, Upstate Biotechnology) diluted 1:500, the KM140 mouse monoclonal antibody specific for Bbc3 diluted 1:50, or a mouse monoclonal anti-cytochrome *c* antibody (clone 6H2.B4, #65971; BD Biosciences) diluted 1:1,000 were used to detect the respective proteins. After washing, biotin-conjugated anti–mouse or anti–rabbit IgG (1:1,000; Vector Laboratories) was added for 1 h, followed by a 20 min treatment with streptavidin-Oregon green conjugate (1 μg/ml; Molecular Probes, Inc.). In case of the cytochrome *c* staining, a Texas red–coupled anti–mouse antibody was used (T-0300; Molecular Probes, Inc.). As a negative control, cultures were incubated with the secondary antibody only. Fluorescence was observed using an inverted microscope (Eclipse TE300; Nikon). Digital images of equal exposure were acquired with the SPOT-2 camera using SPOT software version 2.2.1 (Diagnostic Instruments). Nuclei were stained with Hoechst 33258 (1 μg/ml in PBS) for 20 min.

Statistics
Data are given as means ± SEM. For statistical comparison, *t* test or one-way ANOVA followed by Tukey test were used. P values smaller than 0.05 were considered to be statistically significant.

References

Annis, M.G., N. Zamzami, W. Zhu, L.Z. Penn, G. Kroemer, B. Leber, and D.W. Andrews. 2001. Endoplasmic reticulum localized Bcl-2 prevents apoptosis when redistribution of cytochrome c is a late event. *Oncogene.* 20:1939–1952.

Barone, M.V., A. Crozat, A. Tabaee, L. Philipson, and D. Ron. 1994. CHOP (GADD153) and its oncogenic variant, TLS-CHOP, have opposing effects on the induction of G1/S arrest. *Genes Dev.* 8:453–464.

Bouillet, P., D. Metcalf, D.C. Huang, D.M. Tarlinton, T.W. Kay, F. Kontgen, J.M. Adams, and A. Strasser. 1999. Proapoptotic Bcl-2 relative Bim required for certain apoptotic responses, leukocyte homeostasis, and to preclude autoimmunity. *Science.* 286:1735–1738.

DeGracia, D.J., R. Kumar, C.R. Owen, G.S. Krause, and B.C. White. 2002. Molecular pathways of protein synthesis inhibition during brain reperfusion: implications for neuronal survival or death. *J. Cereb. Blood Flow Metab.* 22:127–141.

Desagher, S., and J.C. Martinou. 2000. Mitochondria as the central control point of apoptosis. *Trends Cell Biol.* 10:369–377.

Desagher, S., A. Osen-Sand, A. Nichols, R. Eskes, S. Montessuit, S. Lauper, K. Maundrell, B. Antonsson, and J.C. Martinou. 1999. Bid-induced conformational change of Bax is responsible for mitochondrial cytochrome *c* release during apoptosis. *J. Cell Biol.* 144:891–901.

Fischer, H., U. Koenig, L. Eckhart, and E. Tschachler. 2002. Human caspase 12 has acquired deleterious mutations. *Biochem. Biophys. Res. Commun.* 293:722–726.

Häcki, J., L. Egger, L. Monney, S. Conus, T. Rosse, I. Fellay, and C. Borner. 2000. Apoptotic crosstalk between the endoplasmic reticulum and mitochondria controlled by Bcl-2. *Oncogene.* 19:2286–2295.

Han, J., C. Flemington, A.B. Houghton, Z. Gu, G.P. Zambetti, R.J. Lutz, L. Zhu, and T. Chittenden. 2001. Expression of bbc3, a pro-apoptotic BH3-only gene, is regulated by diverse cell death and survival signals. *Proc. Natl. Acad. Sci. USA.* 98:11318–11323.

Hojmann Larsen, A., A. Frandsen, and M. Treiman. 2001. Upregulation of the SERCA-type Ca²⁺ pump activity in response to endoplasmic reticulum stress in PC12 cells. *BMC Biochem.* 2:4.

Huang, D.C., and A. Strasser. 2000. BH3-only proteins-essential initiators of apoptotic cell death. *Cell.* 103:839–842.

Kaufman, R.J. 1999. Stress signaling from the lumen of the endoplasmic reticulum: coordination of gene transcriptional and translational controls. *Genes Dev.* 13:1211–1233.

Kögel, D., C. Reimertz, H. Düssmann, P. Mech, K.H. Scheidtmann, and J.H. Prehn. 2003. The death associated protein (DAP) kinase homologue Dlk/ZIP kinase induces p19ARF- and p53-independent apoptosis. *Eur. J. Cancer.* 39:249–256.

Luetjens, C.M., S. Lankiewicz, N.T. Bui, A.J. Krohn, M. Poppe, and J.H. Prehn. 2001. Up-regulation of Bcl-xL in response to subtoxic beta-amyloid: role in neuronal resistance against apoptotic and oxidative injury. *Neuroscience.* 102:139–150.

Muthukkumar, S., P. Nair, S.F. Sells, N.G. Maddiwar, R.J. Jacob, and V.M. Rangnekar. 1995. Role of EGR-1 in thapsigargin-inducible apoptosis in the melanoma cell line A375-C6. *Mol. Cell. Biol.* 15:6262–6272.

Nakagawa, T., and J. Yuan. 2000. Cross-talk between two cysteine protease families. Activation of caspase-12 by calpain in apoptosis. *J. Cell Biol.* 150:887–894.

Nakagawa, T., H. Zhu, N. Morishima, E. Li, J. Xu, B.A. Yankner, and J. Yuan. 2000. Caspase-12 mediates endoplasmic-reticulum-specific apoptosis and cytotoxicity by amyloid-beta. *Nature.* 403:98–103.

Nakano, K., and K.H. Vousden. 2001. PUMA, a novel proapoptotic gene, is induced by p53. *Mol. Cell.* 7:683–694.

Okada, T., H. Yoshida, R. Akazawa, M. Negishi, and K. Mori. 2002. Distinct roles of activating transcription factor 6 (ATF6) and double-stranded RNA-activated protein kinase-like endoplasmic reticulum kinase (PERK) in transcription during the mammalian unfolded protein response. *Biochem J.* 366:585–594.

Paschen, W., and A. Frandsen. 2001. Endoplasmic reticulum dysfunction–a common denominator for cell injury in acute and degenerative diseases of the brain? *J. Neurochem.* 79:719–725.

Perez-Sala, D., and F. Mollinedo. 1995. Inhibition of N-linked glycosylation induces early apoptosis in human promyelocytic HL-60 cells. *J. Cell. Physiol.* 163:523–531.

Plemper, R.K., S. Bohmler, J. Bordallo, T. Sommer, and D.H. Wolf. 1997. Mutant analysis links the translocon and BiP to retrograde protein transport for ER degradation. *Nature.* 388:891–895.

Plesnila, N., S. Zinkel, D.A. Le, S. Amin-Hanjani, Y. Wu, J. Qiu, A. Chiarugi, S.S. Thomas, D.S. Kohane, S.J. Korsmeyer, and M.A. Moskowitz. 2001. BID mediates neuronal cell death after oxygen/glucose deprivation and focal cerebral ischemia. *Proc. Natl. Acad. Sci. USA.* 98:15318–15323.

Poppe, M., C. Reimertz, G. Münstermann, D. Kögel, and J.H. Prehn. 2002. Ceramide-induced apoptosis of D283 medulloblastoma cells requires mitochondrial respiratory chain activity but occurs independently of caspases and is not sensitive to Bcl-xL overexpression. *J. Neurochem.* 82:482–494.

Putcha, G.V., K.L. Moulder, J.P. Golden, P. Bouillet, J.A. Adams, A. Strasser, and E.M. Johnson. 2001. Induction of BIM, a proapoptotic BH3-only BCL-2 family member, is critical for neuronal apoptosis. *Neuron.* 29:615–628.

Rami, A., R. Agarwal, G. Botez, and J. Winckler. 2000. mu-Calpain activation, DNA fragmentation, and synergistic effects of caspase and calpain inhibitors in protecting hippocampal neurons from ischemic damage. *Brain Res.* 866:299–312.

Ron, D., and J.F. Habener. 1992. CHOP, a novel developmentally regulated nuclear protein that dimerizes with transcription factors C/EBP and LAP and functions as a dominant-negative inhibitor of gene transcription. *Genes Dev.* 6:439–453.

Sherman, M.Y., and A.L. Goldberg. 2001. Cellular defenses against unfolded proteins: a cell biologist thinks about neurodegenerative diseases. *Neuron.* 29:15–32.

Smith, M.L., G. Bendek, N. Dahlgren, I. Rosen, T. Wieloch, and B.K. Siesjo. 1984. Models for studying long-term recovery following forebrain ischemia in the rat. 2. A 2-vessel occlusion model. *Acta. Neurol. Scand.* 69:385–401.

Ubeda, M., X.Z. Wang, H. Zinszner, I. Wu, J.F. Habener, and D. Ron. 1996. Stress-induced binding of the transcriptional factor CHOP to a novel DNA control element. *Mol. Cell. Biol.* 16:1479–1489.

Wang, X.Z., M. Kuroda, J. Sok, N. Batchvarova, R. Kimmel, P. Chung, H. Zinszner, and D. Ron. 1998. Identification of novel stress-induced genes downstream of chop. *EMBO J.* 17:3619–3630.

Wei, M.C., W.X. Zong, E.H. Cheng, T. Lindsten, V. Panoutsakopoulou, A.J. Ross, K.A. Roth, G.R. MacGregor, C.B. Thompson, and S.J. Korsmeyer. 2001. Proapoptotic BAX and BAK: a requisite gateway to mitochondrial dysfunction and death. *Science.* 292:727–730.

Whitfield, J., S.J. Neame, L. Paquet, O. Bernard, and J. Ham. 2001. Dominant-negative c-Jun promotes neuronal survival by reducing BIM expression and inhibiting mitochondrial cytochrome c release. *Neuron.* 29:629–643.

Wiertz, E.J., D. Tortorella, M. Bogyo, J. Yu, W. Mothes, T.R. Jones, T.A. Rapoport, and H.L. Ploegh. 1996. Sec61-mediated transfer of a membrane protein from the endoplasmic reticulum to the proteasome for destruction. *Nature.* 384:432–438.

Wobser, H., H. Düssmann, D. Kögel, H. Wang, C. Reimertz, C.B. Wollheim, M.M. Byrne, and J.H. Prehn. 2002. Dominant-negative suppression of HNF-1 alpha results in mitochondrial dysfunction, INS-1 cell apoptosis, and increased sensitivity to ceramide-, but not to high glucose-induced cell death. *J. Biol. Chem.* 277:6413–6421.

Yan, S.F., T. Fujita, J. Lu, K. Okada, Y. Shan Zou, N. Mackman, D.J. Pinsky, and D.M. Stern. 2000. Egr-1, a master switch coordinating upregulation of divergent gene families underlying ischemic stress. *Nat. Med.* 6:1355–1361.

Yu, J., L. Zhang, P.M. Hwang, K.W. Kinzler, and B. Vogelstein. 2001. PUMA induces the rapid apoptosis of colorectal cancer cells. *Mol. Cell.* 7:673–682.

Yu, J., Z. Wang, K.W. Kinzler, B. Vogelstein, and L. Zhang. 2003. PUMA mediates the apoptotic response to p53 in colorectal cancer cells. *Proc. Natl. Acad. Sci. USA.* 100:1931–1936.

Zinszner, H., M. Kuroda, X. Wang, N. Batchvarova, R.T. Lightfoot, H. Remotti, J.L. Stevens, and D. Ron. 1998. CHOP is implicated in programmed cell death in response to impaired function of the endoplasmic reticulum. *Genes Dev.* 12:982–995.